S region sequence, RNA polymerase II, and histone modifications create chromatin accessibility during class switch recombination

Lili Wang,[1] Robert Wuerffel,[1] Scott Feldman,[1] Ahmed Amine Khamlichi,[2] and Amy L. Kenter[1]

[1]Department of Microbiology and Immunology, University of Illinois College of Medicine, Chicago, IL 60612
[2]Université Paul Sabatier, III, Centre National de la Recherche Scientifique, Unite Mixte de Recherche 5089–Institut de Pharmacologie et de Biologie Structurale, 31077 Toulouse Cedex, France

Immunoglobulin class switch recombination is governed by long-range interactions between enhancers and germline transcript promoters to activate transcription and modulate chromatin accessibility to activation-induced cytidine deaminase (AID). However, mechanisms leading to the differential targeting of AID to switch (S) regions but not to constant (C_H) regions remain unclear. We show that S and C_H regions are dynamically modified with histone marks that are associated with active and repressed chromatin states, respectively. Chromatin accessibility is superimposable with the activating histone modifications, which extend throughout S regions irrespective of length. High density elongating RNA polymerase II (RNAP II) is detected in S regions, suggesting that the transcription machinery has paused and stalling is abolished by deletion of the S region. We propose that RNAP II enrichment facilitates recruitment of histone modifiers to generate accessibility. Thus, the histone methylation pattern produced by transcription localizes accessible chromatin to S regions, thereby focusing AID attack.

CORRESPONDENCE
Amy L. Kenter:
star1@uic.edu

Abbreviations used: Ac, acetylation; AID, activation-induced cytidine deaminase; C_H, constant; ChIP, chromatin immunoprecipitation; CSR, class switch recombination; DC-PCR, digestion circularization PCR; DSB, double-strand break; GLT, germline transcript; H3Ac, acetylated histone H3K9,K14; HAT, histone acetyltransferase; HDAC, histone deacetylase; HMT, histone methyltransferase; Me, methylation; PST, postswitch transcript; qPCR, quantitative real-time PCR; qRT-PCR, quantitative real-time RT-PCR; RES, restriction sensitivity endonuclease; RNAP II, RNA polymerase II; S, switch; TSA, trichostatin A; TSS, transcription start site.

Immunoglobulin class switch recombination (CSR) occurs in mature B cells and promotes diversification of effector functions encoded in constant (C_H) regions while maintaining the original antigen-binding specificity arising from V(D)J recombination. The mouse *Igh* locus contains eight C_H genes (μ, δ, γ3, γ1, γ2a, γ2b, ε, and α) that are located downstream of the V, D, and J_H segments, and each C_H region is paired with a complementary switch (S) region (with the exception of Cδ). CSR occurs through an intrachromosomal deletional rearrangement that results in the formation of composite Sμ–Sx junctions on the chromosome, whereas the intervening genomic material is looped out and excised. Long-range interactions between transcriptional regulatory elements in the *Igh* locus form a unique chromosomal loop that facilitates S–S synapsis before CSR (Wuerffel et al., 2007). Activation-induced cytidine deaminase (AID) is required for CSR (Muramatsu et al., 2000) and initiates S region–specific double-strand breaks (DSBs) that are processed through a cascade of events mediated by nonhomologous end joining (Kenter, 2005; Chaudhuri et al., 2007).

The mechanism by which AID is globally targeted to Ig genes and specifically focused on S regions to the exclusion of C_H regions remains unclear. The specificity of AID for single-stranded DNA templates (Chaudhuri et al., 2007) requires that substrate becomes accessible in chromatin before CSR. Targeting of particular S regions for CSR is dependent on expression of germline transcripts (GLTs), which initiate at the I exon and traverse the S and C_H regions (Manis et al., 2002). However, it is unknown whether the distribution of histone modifications created during transcription determine zones of chromatin accessibility in S regions that are amenable to AID attack. This is an intriguing question because S regions can extend >10 kb from the GLT promoter and, yet, are likely to be accessible and to engage in CSR throughout their entire length,

L. Wang's present address is Cancer Vaccine Center, Dept. of Medical Oncology, Dana-Farber Cancer Institute, Boston, MA 02115.

The Rockefeller University Press $30.00
J. Exp. Med. Vol. 206 No. 8 1817-1830
www.jem.org/cgi/doi/10.1084/jem.20081678

The Journal of Experimental Medicine

as indicated by the distribution of recombination breakpoints across S regions (Gritzmacher, 1989).

Chromatin alterations involving ATP-dependent remodeling of nucleosomes and posttranslational modifications on core histones can affect sequence accessibility for DNA binding proteins or create a versatile code for recruitment of factors that control transcription, replication, recombination, and DNA repair (Groth et al., 2007; Kouzarides, 2007; Li et al., 2007). Genome-wide analyses indicate that promoter-proximal sites are enriched with histones that are hyperacetylated and trimethylated on histone H3 at lysine 4 (H3K4me3), and with initiating RNA polymerase II (RNAP II) phosphorylated at serine 5 (p-ser5), whereas levels of H3K36me3 and elongating RNAP II p-ser2 are elevated in the downstream coding regions of active genes (Bernstein et al., 2005; Pokholok et al., 2005; Barski et al., 2007; Guenther et al., 2007). Histone acetylation (Ac) is generally considered an excellent marker of chromatin accessibility. Accessibility may be generated by charge change, which releases the electrostatic grip of histones on DNA and/or creates new binding surfaces for bromodomains contained within many chromatin-modifying proteins (for review see Shahbazian and Grunstein, 2007). Studies in yeast demonstrate that a protein integral to the NuA3 histone acetyltransferase (HAT) complex binds with H3K4me3, indicating a mechanistic link between H3K4 methylation (Me) and histone hyper-Ac (Taverna et al., 2006). In contrast, H3K36me3 is recognized by a subunit of the histone deacetylase (HDAC) Rpd3S, thereby deacetylating the downstream coding regions and suppressing spurious transcription initiation in the wake of elongating RNAP II (Lieb and Clarke, 2005). By these mechanisms, maximum chromatin accessibility is focused to promoter-proximal regions, whereas repressed chromatin is found in downstream coding regions.

In this paper, we show that S regions are hyperaccessible, whereas C_H regions are relatively inaccessible in chromatin of activated B cells. Multiple chromatin modifications were analyzed by chromatin immunoprecipitation (ChIP) in three I-S-C_H regions of the *Igh* locus during CSR in vivo. Unexpectedly, the 3′ boundary of H3K4 Me and histone Ac modifications was located at the 3′ end of S regions irrespective of length, which vary from 1 to 10 kb. We demonstrate that elongating RNAP II p-ser 5 becomes enriched across transcriptionally active S regions, whereas pausing is not detected in the absence of an S region. Similarly, the extended distribution of H3K4me3 across the Sμ region is absent in B cells harboring a targeted deletion of this S region. Thus, the unique sequence of S regions determines the pattern of RNAP II distribution and associated chromatin modifications that ensure maximum chromatin accessibility.

RESULTS

S region hyperaccessibility is transcription dependent and B cell specific

To investigate whether there is a differential pattern of chromatin accessibility associated with S and C_H regions, we designed restriction sensitivity endonuclease (RES) assays that were used in conjunction with the 1.B4.B6 cell line capable of inducible CSR (Ma et al., 2002; Wang et al., 2006). The RES assay is a sensitive method for monitoring nucleosome positioning and remodeling events at punctate sites within a locus. Unstimulated 1.B4.B6 cells express only μ GLTs, whereas stimulation with LPS, CD40L, and IL-4 for 48 h leads to enhanced production of μ, γ1, and ε GLTs as compared with the *Gapd* loading control (Fig. 1 A, left), as expected (Ma et al., 2002; Wang et al., 2006). The postswitch transcript (PST) expression profile, an indicator of successful CSR, was analyzed after 5 d of stimulation and tightly recapitulated the GLT expression pattern (Fig. 1 A, right; Ma et al., 2002).

Nuclei from unstimulated and LPS+CD40L+IL-4–stimulated 1.B4.B6 cells were treated with a limiting and fixed concentration of Hind III for increasing periods of time, including 1, 5, and 15 min. After purification of genomic DNA, the efficiency of cleavage in isolated nuclei was monitored by semi-quantitative ligation-mediated PCR reactions that detect specific cleavage products. A standard curve was developed to establish the linear range of detection for the assay using genomic DNA digested to completion in vitro and referred to as "input" DNA. We first probed chromatin accessibility at two Hind III restriction sites that lie immediately upstream of Sμ and within Cμ using primer sets Sμ-U.A and Cμ.A, respectively (Fig. 2 A). The Hind III site at the 5′ end of Sμ was efficiently cleaved, but the site within Cμ was largely resistant to cutting in both unstimulated and activated cells (Fig. 1 B). Equivalent amounts of cleaved chromatin were used, as indicated by PCR amplification of the *Gapd* gene (Fig. 1 B). These results cannot be attributed to poor Cμ.A primer efficiency, because the Sμ-U.A and Cμ.A primers produced similar levels of PCR products when using input DNA (Fig. 1 B). Because the Cμ cleavage product was only evident after 15 min of digestion with Hind III, we chose the 1- and 15-min digestion periods as standards for subsequent studies.

To extend these analyses, we performed RES assays using nuclei from LPS-activated splenic B cell cultures. Isotype switching is a dynamic process in B cells that is dependent on GLT and AID expression, DSB formation specific to S regions, and proliferation (Kenter, 2005; Chaudhuri et al., 2007). AID is expressed 48 h after LPS activation but CSR has not yet transpired (Wuerffel et al., 2007). Therefore, analyses reported were performed on B cells activated for 48 h or less. B cells were successfully induced, as determined by the induction of AID and GLTs after 48 h of stimulation with LPS or LPS+IL-4 as assessed by quantitative real-time PCR (qPCR; Fig. 1 C, top), and essentially identical results for GLTs were found at 24 h of activation (Wang et al., 2006). The γ3 GLTs were induced by LPS activation and were suppressed by LPS+IL-4 treatment, whereas the γ1 and ε GLT expression were LPS+IL-4 dependent. The PST expression profile was highly correlated with the expression of GLTs and AID (Fig. 1 C, bottom).

Next, we performed RES assays for five Hind III restriction sites, flanking the Sμ and Cμ regions (Sμ-U.A and Sμ-D.A Cμ.A) and the Sγ3 and Cγ3 regions (Sγ3-D.A and Cγ3-D.A; Fig. 2, A and B). Our approach allows a direct comparison of

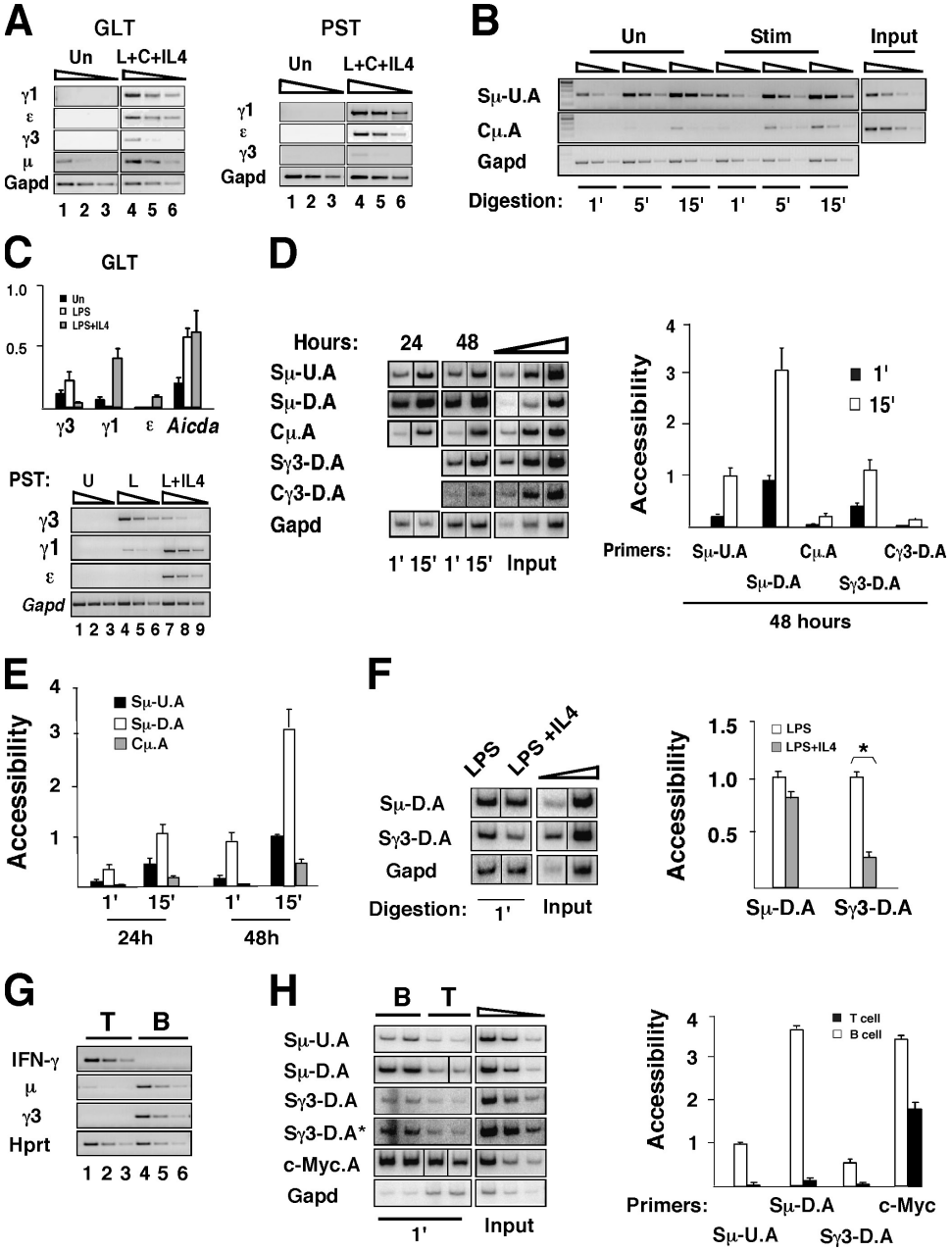

Figure 1. S regions become hyperaccessible in LPS-activated B cells and a B cell line. (A) GLTs and PSTs were analyzed by semiquantitative RT-PCR using cDNAs derived from 1.B4.B6 cells that were either unstimulated (Un) or activated with LPS+CD40L+IL-4 (L+C+IL-4) for 48 h and 5 d, respectively. (B) Nuclei from 1.B4.B6 cells were digested with Hind III for 1, 5, and 15 min (′), and cleavages at the Sμ-U.A and Cμ.A sites were analyzed by RES assay. PCR amplification of the *Gapd* gene is used as a loading control. The linearity of each assay was demonstrated by fourfold serial dilutions of genomic DNA cut to completion in vitro (Input). (C) Splenic B cells were unstimulated or activated with LPS or LPS+IL-4. Activation was performed for 48 h or 5 d, and cDNAs were derived for GLT in qRT-PCR or PST in semiquantitative RT-PCR analyses, respectively. The relative transcript levels for GLT and PST are normalized to *Hprt* (top) or *Gapd* (bottom), respectively. SEMs are shown. (D and E) Splenic B cells activated with LPS for 24 or 48 h, as indicated, were analyzed using RES assays, and digestion was performed for 1 or 15 min, as indicated. All PCR amplification products were in the linear range of detection as compared with standard curves for each primer set (Input). The concentration of PCR products was normalized with the *Gapd* loading control, and the relative accessibility was calculated. The results from four samples derived from two independent experiments are shown with SEMs. (E) Cleavage (15′) at the Sμ-U.A site was arbitrarily set to 1. (F) B cells stimulated with LPS or LPS+IL-4 were analyzed using RES assays at the Sμ-D.A and Sγ3-D.A sites using a cleavage time of 1 min. Cleavage in the LPS-stimulated samples was arbitrarily set to 1, and SEMs are shown. The one-tailed Student's *t* test was used to determine the significance of the difference between stimulated samples (*, $P < 0.05$). (G) Splenic B and T cells were activated with LPS or concanavalin A for 48 h, respectively. GLTs (μ and γ3) and IFN-γ expression were analyzed by semiquantitative RT-PCR. (H) RES assays were performed with the indicated primer sets using three independent samples analyzed in duplicate and a digestion time of 1 min. In the gel image, Sγ3-D.A* is a longer exposure of Sγ3-D.A (left). Cleavage at the Sμ-U.A site was set to 1 in B cells (right), and data are shown with SEMs. Black lines indicate that intervening lanes have been spliced out.

accessibility at all five sites and demonstrates that in LPS-activated B cells, the Sμ and Sγ3 regions are 2–35-fold more susceptible to cleavage than Cμ or Cγ3 after 15 min of Hind III digestion (Fig. 1 D). The level of accessibility for Sμ-D.A is fourfold higher than that found for Sμ-U.A, which may be caused by differences in nucleosome phasing at these sites in the transcriptionally active μ locus. Because histone Ac at S regions accumulates with increasing periods of B cell activation (Wang et al., 2006), we examined the cleavage of these sites in B cells that were activated with LPS for 24 and 48 h. At both time points, there was preferential accessibility at sites flanking Sμ as compared with Cμ and accessibility progressed over time (Fig. 1 E), demonstrating a correlation between the observed kinetics of histone Ac (Wang et al., 2006) and hyperaccessibility at Sμ and Sγ3 regions.

To determine whether S region accessibility is contingent on GLT expression, we monitored changes in chromatin cleavage at the Sμ and Sγ3 regions in B cells activated with LPS or LPS+IL-4 for 48 h in RES assays. The γ1 locus was not amenable to this analysis because it lacks appropriately positioned Hind III sites (Fig. 2 C). B cell activation with LPS+IL-4 suppresses γ3 GLT expression four- to fivefold as compared with that found in LPS-activated B cells and shifts switching from μ→γ3 to μ→γ1 (Fig. 1 C). Consistent with the GLT expression profile, cleavage was suppressed threefold at the Sγ3-D.A site in response to LPS+IL-4 as compared with that found after LPS induction, and this difference was statistically significant ($P < 0.05$; Fig. 1 F). In contrast, essentially no change in the level of cleavage was found at the comparable location downstream of Sμ when the cells were activated with either LPS or LPS+IL-4. The Sμ region is the universal donor in CSR and is used in both μ→γ3 and μ→γ1 CSR. Thus, chromatin remodeling at the Sγ3 region is tightly correlated with the expression of the γ3 GLT.

To further confirm the relevance of the in vivo RES assay, we compared the level of S region accessibility in splenic B cells capable of inducing CSR and T cells that are incapable of this function. Expression of μ and γ3 GLT and the IFN-γ genes from LPS- and concanavalin A–activated B and T cells, respectively, demonstrates successful cellular activation (Fig. 1 G). RES analyses indicate that Hind III sites in Sμ and Sγ3 regions were 15–60-fold more efficiently cleaved in B cells than in T cells (Fig. 1 H). The difference in the level of S region accessibility cannot be attributed to global differences in the efficiency of Hind III digestion in B and T cells, because the levels of cutting at a Hind III site in the ubiquitously expressed *c-myc* gene differed by only twofold. Cumulatively, these findings demonstrate that chromatin remodeling at the boundaries of S regions is inducible, transcription dependent, and specific to B lymphocytes.

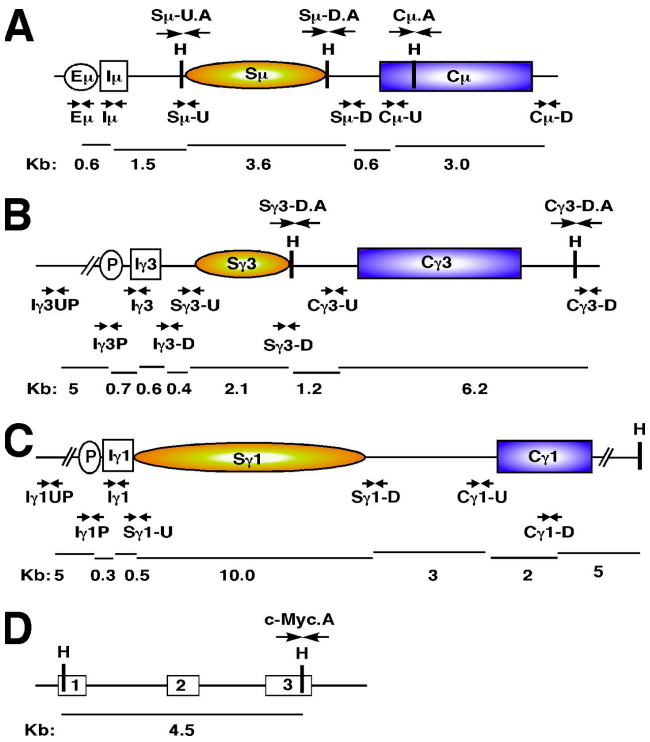

Figure 2. Schematic diagrams for each of the μ, γ3, and γ1 I-S-C_H loci and the *c-myc* gene are shown. Vertical lines indicate Hind III (H) sites. The arrows above and below the line show primer pairs used in the RES and ChIP assays, respectively. The distance between primer sets is shown (kb) under the horizontal bars. (A–C) The μ, γ3, and γ1 I-S-C_H loci include the GLT promoter (P), the I exon (I), the C_H (C) region, and the μ intronic enhancer (Eμ) in the μ locus. (D) The schematic for the three exons of the *c-myc* gene are indicated by the numbered boxes.

S regions targeted for CSR are hyperacetylated at histone H3K9,14

The RES assay has the potential to reveal punctate chromosomal alterations induced by both ATP-dependent remodeling complexes as well as histone modifiers. To test the proposition that inducible histone modifications contribute to the differential accessibility of S and C_H regions to AID attack, ChIP assays were performed. ChIP assays measure the mean levels of chromatin modifications that are associated with the active or repressed chromatin states over several hundred bp. We investigated whether Ac histones are evenly distributed throughout the μ, γ3, and γ1 I-S-C_H loci or are locally constrained to specific subregions in activated B cells. ChIP analyses were performed using antibodies to acetylated histone H3K9,K14 (H3Ac) in combination with primer pairs spanning the μ, γ3, and γ1 I-S-C_H loci (Fig. 2, A–C; Table I; Wang et al., 2006), and were assessed by qPCR. Primers located within S regions are difficult to design because of the reiterative composition of these DNA sequences.

Our earlier studies indicate that there are three layers of regulation controlling histone Ac at S regions: B cell activation, transcription, and AID expression leading to DSB formation (Wang et al., 2006). At the μ locus and in accordance with our previous findings, H3Ac modifications are detectable in unstimulated B cells and are further induced by both LPS or LPS+IL-4, whereas this activation treatment did not lead to a significant change in the steady-state level of μ GLT (Fig. 3; Wang et al., 2006). The highest levels of H3Ac were

found over the Sμ region and dropped sharply at 3′ Sμ and Cμ (Fig. 3). The relatively high level of H3Ac in unstimulated B cells is consistent with the constitutive transcription of the μ H chain and Iμ-Cμ GLT in these cells. Consistent results were obtained for four to six ChIP samples from two independent experiments that were assayed in duplicate. Additional studies using B cells activated with LPS or LPS+IL-4 and newly designed primers sets, Sμ-D.1 and Sμ-D.2 that overlap with the Sμ-D.A site analyzed in RES assays, indicated that the zone of hyper-H3Ac extends to the 3′ end of the Sμ tandem repeats (Figs. 2; and 4, A and B). Although the magnitude of H3Ac increase at Sμ region boundaries is roughly equivalent (Fig. 4 B, compare Sμ-U and Sμ-D.2), restriction enzyme accessibility is about fourfold higher at the 3′ end of Sμ (Fig. 1, D, E, and H), suggesting that remodeling at this downstream site may be less dependent on H3Ac and more related to nucleosome phasing. Despite these intralocus differences, the chromatin at sites surrounding Sμ is far more

Table I. Primers used in ChIP, RES, RT-PCR, and DC-PCR analyses

Primer	Forward (5′ to 3′)	Reverse (5′ to 3′)
ChIP assays		
Eμ	GGGAGTGAGGCTCTCTCATA	ACCACAGCTACAAGTTTACCTA
Iμ	CTTCCCTCTGATTATTGGTCTCCA	CTCAACCACCAACCAGCATG
Sμ-U	TCTAAAATGCGCTAAACTGAGG	AGCGTAGCATAGCTGAGCTC
Sμ-D	CTGAATGAGTTTCACCAGGCC	GGCCTGTCCTGCTTGGCTTC
Sμ-D.1	GGGGTGAGCCGGGATGTTTT	AGCCAGCTCTACTCACTCTT
Sμ-D.2	GCTGACATGGATTATGTGAGG	CCTACACCAGATCATCCAGTACAGCT
Cμ-U	CTTCCCAAATGTCTTCCCCC	TGCGAGGTGGCTAGGTACTTG
Cμ-D	TAACACTGCCTCTTTGGGCTC	TGCTTGTCCTACCCCTGCC
Iγ1-UP	TGTTGGGCACCATTTTGTTG	AGCACATGGCCTGGAGAAAC
Iγ1-P	GAGTCTCAAGGGTACCGCCTCA	CAGAGTCACAGCCTTTGTCCCA
Iγ1	TATGATGGAAAGAGGTAGCATT	CTGGGCTGGTCTGTCAACTCCTT
Sγ1-U	GGGGGAGGAGATATCCAAGA	CAGCTCTTTTGCAGGTCTTG
Sγ1-D	CAGGCAAACTAAACCAGTGGG	AGGATGTCCACCCTCACCCAGGC
Cγ1-U	GCCCAAACTAACTCCATGGTG	CAACGTTGCAGGTGACGGT
Cγ1-D	CAACACCCTGCCAATAAGGC	CCCACTTGTAAATGCCGAGG
Sγ3-D.1	CAGGCTGGGAAACTCTTGGG	AGGTTAGTCCCCATACTTGAACC
RES assays		
L.1	GGTGACTGCAGAGATCTGAATTCAA	
L.2	AGCTTTGAATTCAGATCTCTGC	
Sμ-U.A (round 1)	L.1	AGCGTAGCATAGCTGAGCTC
Sμ-U.A (round 2)	CTGAATTCAAAGCTTGCTGAGCA	CAGCCTAGTTTAGCTTAGCG
Sμ-D.A (round 1)	L.1	AAGAGTGAGTAGAGCTGGCT
Sμ-D.A (round 2)	CTGCAGAGATCTGAATTCAAAGC	AAGAGTGAGTAGAGCTGGCT
Cμ.A (round 1)	L.1	GATCCCTGTGAGTCACAGTA
Cμ.A (round 2)	CTGAATTCAAAGCTTTTTTCCAAC	CACTAGCCACACCCTTAGCA
Sγ3-D.A (round 1)	L.1	ATGAGGACTAGGTTGGGCAG
Sγ3-D.A (round 2)	CTGAATTCAAAGCTTCTACAAACCT	GGGAGCTGGGGCTATCAGA
Cγ3-D.A (round 1)	L.1	CAGAATGCTGGGTGAGTGGT
Cγ3-D.A (round 2)	CTGAATTCAAAGCTTAGCTTTGCC	TGTGAGTTTTGTACAAGGAG
c-Myc.A (round 1)	L.1	GAAACTCTGGTGCATAAACTGACCTAAC
c-Myc.A (round 2)	GAGATCTGAATTCAAAGCTTACAGTCCC	TCGAGGAGGAGCTGGAATCTCTCGTGA
RT-PCR		
IFN-γ	GGATGCATTCATGAGTATTGC	CCTTTTCCGCTTCCTGAGG
DC-PCR		
μ→γ1 (round 1)	CAGCCTAGTTTAGCTTAGCG	CTCGCAAAAGCAGCATATAC
μ→γ1 (round 2)	GCTCAGCTGTGCTTTTTAGAGCCTCG	CATAGGCAGAACAGCCACAGCTAGAG
μ→γ3 (round 1)	AGCGTAGCATAGCTGAGCTC	GGGAGCTGGGGCTATCAGA
μ→γ3 (round 2)	GCTCAGCTGTGCTTTTTAGAGCCTCG	ACAGGGTCCCAGGTTATGCAG
Gapd (round 1)	TCAACTACATGGTCTACATGTTCC	AATGGAGCCTGGCAGACTGA

accessible than that found in T cells (Fig. 1 H), indicating that Sμ region hyperaccessibility occurs after activation of mature splenic B cells.

We confirm that at the γ3 locus, H3Ac levels increase in response to LPS treatment, peak over Iγ3-Sγ3, and were low at Cγ3 (Fig. 3), as observed previously (Wang et al., 2006). LPS+IL-4 activation led to hypo-H3Ac across the entire γ3 locus (Fig. 3), indicating that chromatin is a relatively inaccessible state when γ3 GLTs are repressed (Figs. 1 C and 3). Conversely, LPS+IL-4 treatment induced histone H3Ac across the Iγ1-Sγ1 region, a distance >10 kb, but levels were significantly reduced when activated by LPS alone, conditions that specifically repress the γ1 GLT and induce μ→γ3 CSR. These findings indicate that chromatin remodeling is targeted to transcriptionally active S regions and is spread throughout the S region irrespective of length. The mechanism that regulates the spread of histone Ac throughout the S regions but spares the C_H regions remains unclear.

Modulation of histone Ac in S regions leads to altered accessibility and CSR frequency

Induced H3Ac in S regions is expected to lead to chromatin hyperaccessibility and increased CSR if H3Ac is physiologically important to the recombination process. To manipulate the level of H3Ac in S regions, splenic B cells were stimulated with LPS or LPS+IL-4 for 48 h in the presence and absence

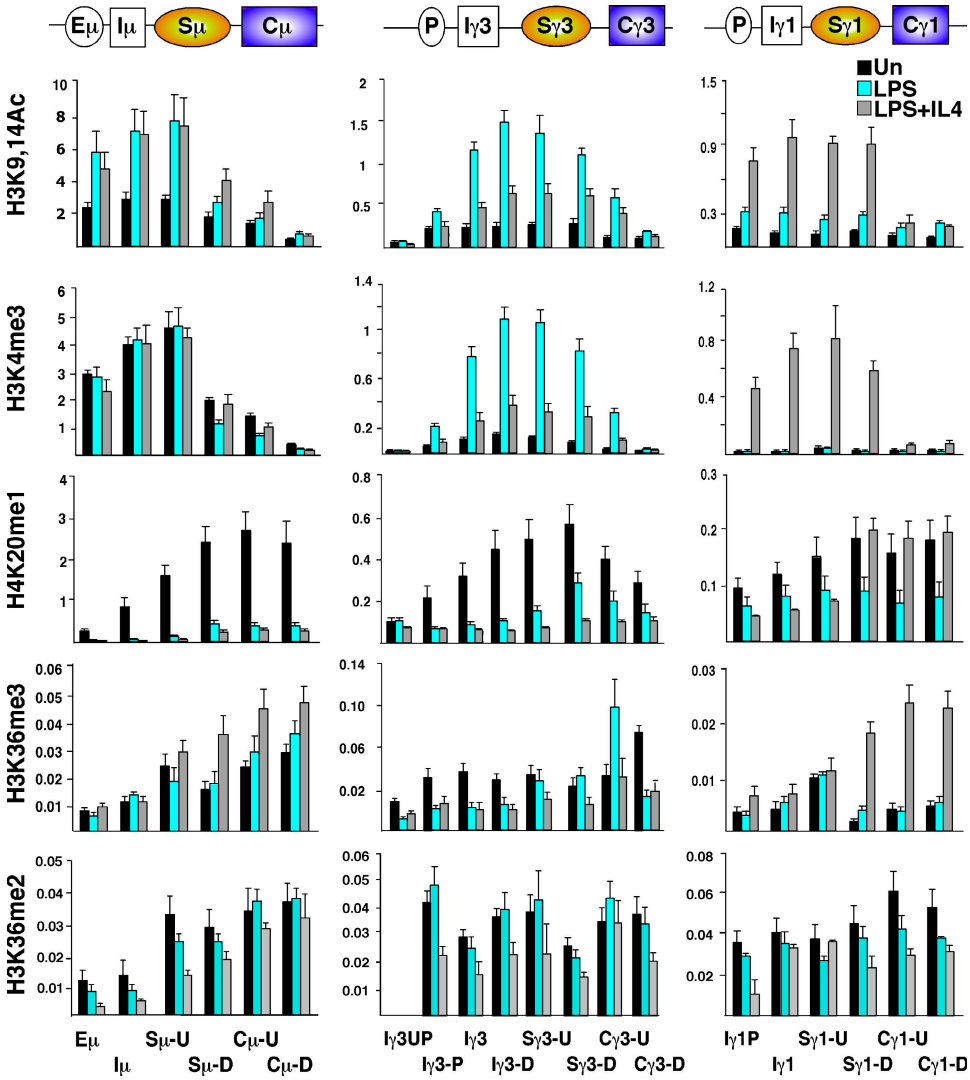

Figure 3. Differential segregation of histone modifications uniquely identify the S and C_H regions in the μ, γ3, and γ1 *Igh* loci. Schematic diagrams for each of the μ, γ3, and γ1 I-S-C_H loci are shown at the top and are aligned appropriately with the sites analyzed by ChIP. Primer pairs used in the ChIP analyses are named below the histograms. The histone modifications tested for each locus are indicated on the left. ChIP assays were performed on nuclei from splenic B cells that were unstimulated or activated with LPS or LPS+ IL-4 for 48 h from four to six samples derived from two independent experiments using anti-H3K9,14Ac (H3Ac), anti-H3K4me3, anti-H3K36me2, anti-H3K36me3, and anti-H4K20me1 antibodies. All samples were analyzed in duplicate and averaged, and SEMs are shown. The fraction of input is calculated as the qPCR product concentration relative to 10% input and indicates the enrichment of a sequence after immunoprecipitation.

of the general HDAC inhibitor trichostatin A (TSA) and analyzed for H3Ac, S region accessibility, and CSR frequency. TSA treatment had little or no effect on the expression of μ, γ3, and γ1 GLTs in response to B cell inducers; thus, transcription is intact (Fig. 4 A). In the Sμ locus, TSA had no effect on H3Ac levels in the area spanning Eμ-Sμ, whereas there was a modest but statistically significant ($P < 0.001$) increase of H3Ac in downstream areas (Fig. 4 B). In the γ3 and γ1 loci,

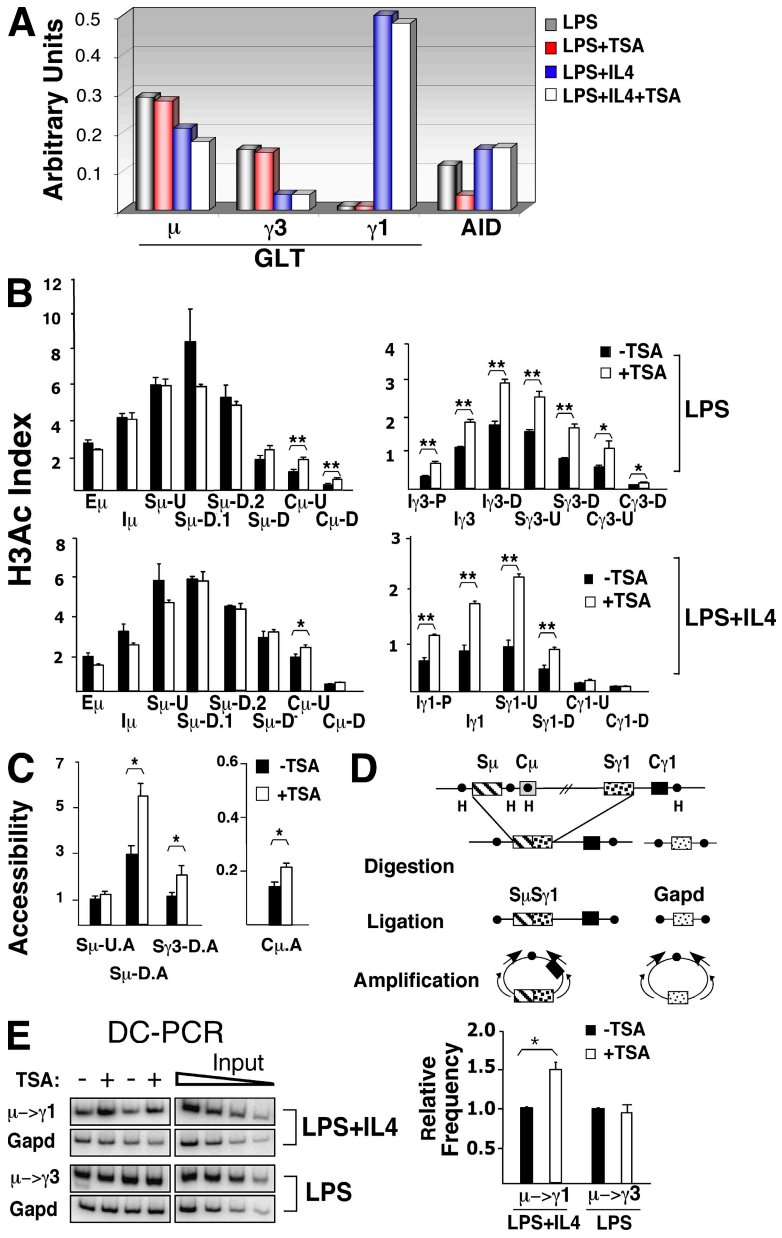

Figure 4. Histone H3Ac in S regions determines chromatin accessibility and CSR frequency. B cells were stimulated with LPS or LPS+IL-4 in the presence or absence of 3 ng/ml TSA for 48 h (A–C) or 5 d (E). (A) GLTs and AID expression were analyzed by qRT-PCR from B cells stimulated as indicated. (B) ChIP assays were performed using anti-H3K9,14Ac antisera and were analyzed by qRT-PCR. H3Ac indices are shown for the μ, γ3, and γ1 loci. Data are averaged from four samples derived from two independent experiments, and SEMs are shown. (B, C, and E) A single-tailed Student's *t* test was used to determine the significance of the differences in samples with or without TSA treatment (*, $P < 0.05$; **, $P < 0.001$). (C) Nuclei from B cells activated with LPS were analyzed using RES assays digested with Hind III for 1 min (1′), and averaged data are shown. Cleavage at the Sμ-U.A site was set to 1. Data for three to four samples derived from two independent experiments were analyzed in duplicate and averaged, and SEMs are shown. (D) A schematic diagram summarizing the DC-PCR assay is shown with nested PCR primers and Hind III sites indicated by the arrows and filled circles, respectively. The *Gapd* gene was used as a control for ligation and DNA loading. (E, left) Representative gel images for the semiquantitative DC-PCR assays are shown. The linearity of each assay was demonstrated by twofold serial dilutions of genomic DNA, as indicated (Input). (right) Relative CSR frequency was calculated by normalizing the DC-PCR product with the *Gapd* loading control. CSR frequency from samples without TSA treatment was set to 1.

TSA treatment caused a clear 1.5–2-fold increase in H3Ac that was statistically significant (p-values ranged from $P < 0.05$ to 0.001) and that spanned the I-S-C_H regions. The TSA hypersensitivity of H3Ac in Sγ regions and the relative insensitivity of Sμ to this treatment may be related to the induced transcription of Sγ loci as compared with the steady-state expression of the μ locus, as has been noted previously (Shahbazian and Grunstein, 2007). In parallel RES analyses, TSA treatment also led to an increase in cleavage at the Sμ-D, Cμ, and Sγ3-D sites ($P < 0.05$; Fig. 4 C). No change in cleavage was evident at the Sμ-U site, where H3Ac levels were also unchanged by TSA treatment (Fig. 4 C). It is possible that at the Sμ-D site TSA treatment indirectly led to the chromatin remodeling observed in the RES assay. These studies reveal that histone Ac levels at downstream Sγ regions are modulated by ongoing histone deacetylation, whereas this connection is not as evident for the Sμ region in which H3Ac levels are insensitive to HDAC inhibition.

To determine the physiological significance of altered histone Ac in S regions, we measured CSR frequency in B cells activated in the presence or absence of TSA using semiquantitative digestion circularization PCR (DC-PCR) (Fig. 4 D). TSA had no effect on AID expression in LPS+IL-4–stimulated B cells, whereas AID expression was inhibited approximately fivefold in LPS-activated cells, where the underlying mechanism of this repression is unknown (Fig. 4 A). In the DC-PCR assay, the nonrearranging *Gapd* gene was used as a control for the digestion and ligation reactions (Fig. 4, D and E). TSA treatment led to a statistically significant 1.5-fold increase ($P < 0.05$) of the μ→γ1 DC-PCR product from LPS+IL-4–activated B cell cultures as compared with untreated samples (Fig. 4 E). In LPS-induced B cells, TSA treatment led to no change in μ→γ3 switching as compared with untreated samples despite a reduction of AID expression, suggesting that increased levels of H3Ac provided additional accessibility and compensated for decreased AID expression (Fig. 4, A, B, and E). Based on these collective findings, we infer the physiological relevance of H3Ac and chromatin accessibility in the S regions to CSR frequency. We conclude that the balance between HAT and HDAC activities influences both histone Ac and chromatin accessibility in Sγ regions but only modestly regulates the spread of H3Ac into C_H loci.

S and C_H regions are distinguished by differential histone Me

Analysis of histone modifications in genome-wide studies have revealed that H3K4me3 overlaps with H3Ac, is highest at the 5′ ends of coding regions, and is positively correlated with gene activity (Bernstein et al., 2005), whereas H3K36me3 is found in the downstream coding regions of active genes (Bernstein et al., 2005; Pokholok et al., 2005; Barski et al., 2007). Previous analyses of H3K36me2 distribution come almost entirely from yeast studies. H3K36me2 modification is evenly distributed throughout the coding regions (Bannister et al., 2005; Pokholok et al., 2005; Rao et al., 2005) and is correlated with transcriptional competence but not with transcription rates (Rao et al., 2005; Youdell et al., 2008). To determine whether an underlying pattern of chromatin Me modifications correlates with the areas within I-S-C_H loci that are subject to histone Ac, H3K4me3 and H3K36me2,3 marks were profiled across the μ, γ3, and γ1 I-S-C_H loci. In activated B cells, the H3K4me3 and H3K36me3 modifications were reciprocally enriched at the 5′ and 3′ ends of all three loci, whereas H3K36me2 was broadly distributed (Fig. 3). In unstimulated B cells, H3K36me2 is present in both the actively transcribed μ locus and inactive γ3 and γ1 loci, and is not further elevated after B cell activation, indicating that the H3K36me2 deposition profile is similar in yeast and B lymphocytes.

In the Iμ-Sμ-Cμ locus, the overall levels of H3K4me3 and H3K36me3 modifications were very similar in stimulated and untreated B cells, consistent with the constitutive transcription of this locus leading to expression of the μ H chain (Fig. 3). However, using a Student's *t* test, we found that there was a statistically significant increase for H3K36me3 at Sμ-D ($P < 0.007$) and a smaller increase at the Cμ-U and Cμ-D sites ($P < 0.049$ and 0.017, respectively) after activation with LPS+IL-4 but not with LPS alone. Increased H3K36me3 levels suggest induced transcription at the μ locus in response to LPS+IL-4 activation. Our previous studies indicated that the μ GLT is not measurably induced by LPS or LPS+IL-4 stimulation, although the methods used for that analysis may not detect small changes of expression (see next section; Wang et al., 2006). In contrast, very low levels of H3K4me3 and H3K36me3 are distributed across the γ3 and γ1 I-S-C_H locus in unstimulated B cells, consistent with their relatively inactive or silent transcriptional status, respectively (Figs. 1 C and 3). Upon B cell activation with LPS or LPS+IL-4, H3K4me3 and H3K36me3 marks are induced, correlated with robust GLT expression, and are spatially differentiated in I-S-C_H loci (Figs. 1 C and 3). The H3K4me3 deposition pattern is essentially superimposable with the pattern of hyper-H3Ac (Figs. 3, 4 B, and 8 C) and in agreement with genome-wide analyses (Bernstein et al., 2005). Surprisingly, both the H3K4me3 and H3Ac modifications extend across the I-S regions irrespective of S region length, which ranges from 2 to 10 kb (Fig. 2, A–C), suggesting that S DNA sequence may play a role in determining the spatial pattern of these chromatin modifications. In contrast, the H3K36me3 mark is preferentially deposited toward the 3′ end of the locus and may have a relatively repressive influence on chromatin accessibility. In the γ3 locus, induction of H3K36me3 is apparent only at the Cγ3-U site, whereas this mark has a broader distribution over the Cμ and Cγ1 regions. Detection of H3K36me3 in Cγ3 is reproducible and transcription dependent, indicating the relevance of this modification. The more limited detection of H3K36me3 in Cγ3 is consistent with this mark locating to exons of 3′ coding regions (Kolasinska-Zwierz et al., 2009). The 3′ skew for H3K36me3 in transcriptionally active loci is contrasted by the broad distribution of the H3K36me2 mark, which is not altered by transcription.

Although H4K20me1 modifications were initially discovered to be associated with facultative heterochromatin

and considered repressive, this mark is also enriched in active genes (Talasz et al., 2005; Vakoc et al., 2006; Barski et al., 2007). We tested whether H4K20me1 displays spatial patterns in I-S-C_H loci in splenic B cells. High levels of H4K20me1 are distributed across the μ, γ3, and γ1 I-S-C_H locus in unstimulated B cells and skewed toward the 3′ end of each locus (Fig. 3). This pattern occurs irrespective of transcriptional status, because μ is constitutively expressed whereas γ3 and γ1 loci are silent. Unexpectedly, we observed a change in the pattern of H4K20me1 deposition from across μ, γ3, and γ1 I-S-C_H in unstimulated B cells to an area downstream of S regions in activated B cells, suggesting that the Me of this histone lysine residue is highly dynamic (Fig. 3). In summary, the induced deposition of histone modifications H3Ac, H3K4me3, H3K36me3, and H4K20me1 is transcription dependent. These chromatin marks display differential spatial patterns with superimposed H3Ac and H3K4me3 marks that extend throughout the I-S interval (Fig. 5). In contrast, H3K36me3 and H4K20me1 are associated with the region downstream of the S regions (Fig. 5). The transition from the activating H3Ac and H3K4me3 modifications associated with chromatin hyperaccessibility to the repressive marks, H3K36me3 and/or H4K20me1, occurs at the 3′ boundary of the three S regions studied (Fig. 5).

RNAP II p-ser 5 is enriched in S regions

In yeast, the H3K4 histone methyltransferase (HMT) binds to initiating RNAP II p-ser 5 and introduces H3K4me3 into promoter-proximal regions (Hampsey and Reinberg, 2003). Genome-wide studies in humans, mice, and yeast confirm the distribution of H3K4me3 to the promoter-proximal areas, suggesting that this mark is targeted to chromatin via a conserved mechanism involving the RNAP II p-ser5 isoform (Bernstein et al., 2005; Pokholok et al., 2005). These observations imply that the extended distribution of H3K4me3 in S regions might derive from high occupancy RNAP II p-ser5. ChIP has been used to determine RNAP II association at specific promoters and transcribed regions and on a genome-wide scale (Muse et al., 2007; Guenther et al., 2007; Zeitlinger et al., 2007). A ChIP signal exclusively at the promoter indicates that RNAP II is poised at this site, whereas if the ChIP signal is found at short distances downstream of the transcription start sites (TSSs) then RNAP II is paused in early elongation (Saunders et al., 2006; for review see Wade and Struhl, 2008). When the transition from transcription initiation to elongation is rapid, RNAP II occupancy will be roughly equivalent across the gene. Alternatively, if the transition is slow then RNAP II levels will be higher at the promoter than in downstream coding regions. To examine this issue in S regions, ChIP assays focused on μ and γ3 I-S-C_H regions were performed using an antibody against total RNAP II or RNAP II p-ser 5 (H14) detected during the early stages of elongation in B cells. The Sμ tandem repeats are located between Sμ-U and Sμ-D.2 sites, whereas Sμ-D is located ∼600 bp downstream and outside the repetitive zone (Fig. 2). There are three documented TSSs for μ GLT, one immediately upstream of the Iμ exon and two that are located 5′ of Sμ (Fig. 6 A; Alt et al., 1982; Nelson et al., 1983; Kuzin et al., 2000). Before B cell activation, relatively low levels of RNAP II were found throughout the μ I-S-C_H locus, consistent with the constitutive expression of the μ GLT (Fig. 6 A) and suggesting rapid transition of RNAP II from transcription initiation to elongation, as has been previously described for some genes (Zeitlinger et al., 2007). After B cell activation, RNAP II occupancy increased across the Iμ-Sμ-Cμ transcription unit, with the greatest gains at the 3′ end of the Sμ tandem repeats, whereas the sites adjacent to Sμ were relatively depleted of RNAP II (Fig. 6 A). The high occupancy of RNAP II p-ser5 at the 3′ end of Sμ occurs at least 3.2 kb downstream of the TSSs and, therefore, may occur through a unique mechanism that is distinct from the pause associated with the transition from promoter-proximal transcription initiation to elongation. Increased RNAP II occupancy at Sμ (Fig. 6 A) with little concomitant change in μ GLT expression (Wang et al., 2006) could occur from increased transcription initiation that rapidly moves off the promoter but stalls in the S region and never completes the μ GLT. Alternatively, transcription initiation at alternative start sites (Fig. 6 A) might occur, thereby increasing transcription but not changing the level of the classical μ GLT. Finally, antisense RNA transcription initiating within the S region (Perlot et al., 2008) might lead to accumulation of RNAP II in Sμ DNA.

Analysis of the γ3 I-S-C_H region in LPS-activated B cells demonstrates that total RNAP II was distributed across the locus, whereas RNAP II p-ser5 occupancy was highest at the

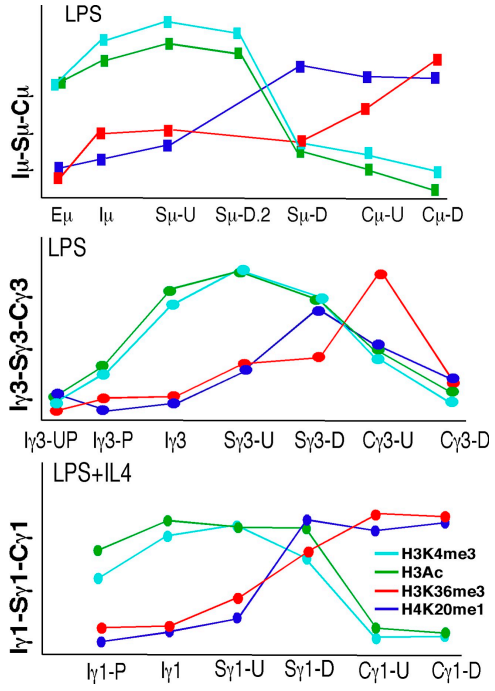

Figure 5. Summary of differential histone modifications in S and C_H regions of activated B cells. B cells were stimulated with LPS or LPS+IL-4 for 48 h and analyzed in ChIP assays using antisera against H3K9,14Ac, H3K4me3, H3K36me3, and H4K20me1. Data were amalgamated from the experiments shown in Figs. 3, 4 B, and 8 C.

Iγ3 exon containing the TSS, and relatively higher levels were also detected within the Sγ3 tandem repeats as compared with the flanking regions (compare Sγ3-D.1 to Sγ3-D; Fig. 6 B). The more significant relative enrichment of RNAP II p-ser5 at Iγ3 as compared with Iμ may arise from the unifocal TSS in the γ3 locus, as compared with three TSSs for the μ GLT and the fact that expression of the γ3 GLT is inducible, whereas the μ GLT is constitutively expressed (Fig. 6 C). RNAP II p-ser5 is abundant in the Sμ and Sγ3, suggesting that S DNA sequence may create an environment that impairs the transition of elongating RNAP II through the region.

RNAP II enrichment does not result from AID-induced DSBs in S regions

One mechanism that could be responsible for RNAP II enrichment is formation of AID-induced DSBs that are targeted to transcribed S regions based on the observation that RNAP I transcription elongation is impeded by DNA breaks (Kruhlak et al., 2007). To determine whether AID-initiated DSBs are responsible for enriched RNAP II through S regions, we compared WT and AID-deficient B cells for RNAP II occupancy using ChIP assays at the Sμ-D.1 and Sμ-D.2 located within the Sμ tandem repeats and Sμ-D situated immediately outside the repeats at the 3′ end of the Sμ region. Appropriate GLT expression was found in response to LPS induction, demonstrating successful B cell activation (Fig. 7 A). In LPS-activated WT and AID-deficient B cells, the total RNAP II density profile across the μ I-S-C_H locus is essentially equivalent (Fig. 7 B). Similarly, the transcription-dependent H3K4me3 profile is essentially identical in WT and AID-deficient B cells, demonstrating that the presence of DSBs in S regions is not a major contributor to RNAP II stalling or H3K4me3 deposition in transcribed S regions (Fig. 7 C). In contrast, histone H3 and H4 Ac is diminished in AID-deficient B cells, suggesting that there are multiple regulators of histone Ac at S regions, including germline transcription, B cell activation, and AID-induced DSB formation (Wang et al., 2006).

S region sequence directs RNAP II occupancy and H3K4me3 distribution

To investigate whether S region sequence contributes to increased RNAP II occupancy and influences the distribution of H3K4me3 modifications, we compared WT and Sμ Δ/Δ mice in which a large portion of the endogenous Iμ-Cμ region including all the Sμ tandem repeats was deleted (Khamlichi et al., 2004), and which is devoid of R-loops in the residual Iμ-Cμ interval (Huang et al., 2007). LPS+IL-4 activation of B cells from WT control or Sμ Δ/Δ mice yielded 48–54% and 12–16% $IgG1^+$ B cells, respectively, demonstrating a four-fold reduction of μ→γ1 CSR in the absence of the Sμ region (Fig. 8 A), whereas no reduction in μ GLT expression has been detected as a consequence of Sμ deletion (Khamlichi et al., 2004). The original characterization of CSR in Sμ Δ/Δ B cells indicated a 20-fold reduction of μ→γ1 switching (Khamlichi et al., 2004). Our current activation conditions (50 μg/ml LPS and 10 ng/ml IL-4) produced switching frequencies that were 2.5-fold higher than those previously reported using lower concentrations of activators (20 μg/ml LPS and 1 ng/ml IL-4; Khamlichi et al., 2004). This level of CSR in the Sμ Δ/Δ B cells is similar to that found for the Sμ tandem repeat–deficient mice in which only the core Sμ region was deleted (Luby et al., 2001).

In the Sμ Δ/Δ locus, the Iμ and Cμ-U or Cμ-D sites are separated by 0.73 or 3.73 kb, respectively, whereas in the

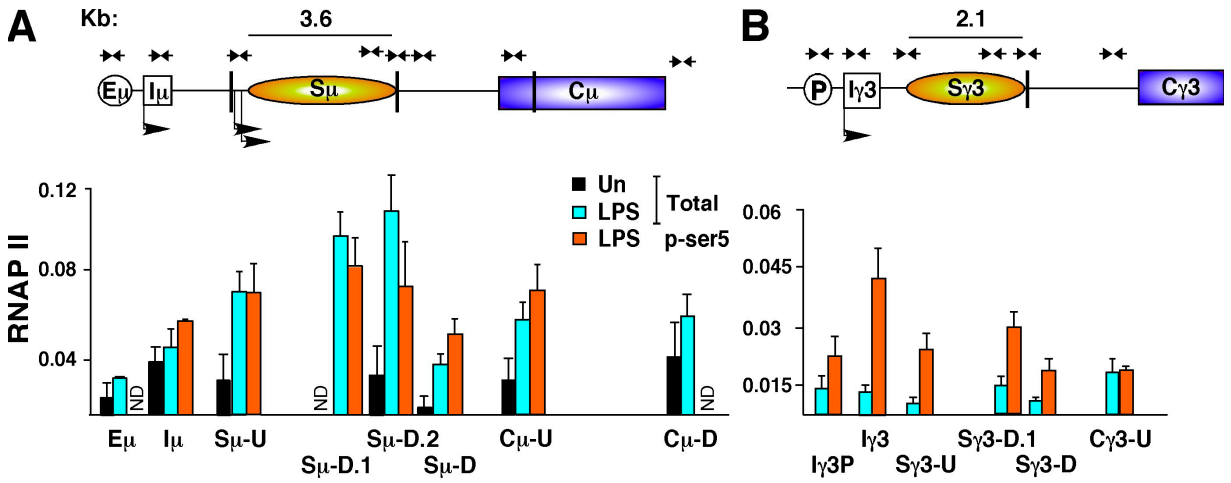

Figure 6. RNAP II p-ser5 is enriched in the Sμ and Sγ3 regions of activated B cells. B cells were stimulated with LPS for 48 h and analyzed in ChIP assays using antisera against total RNAP II or RNAP II CTD p-ser5, as indicated. Primer pairs used in the ChIP analyses are named below the histograms, and their positions in the μ and γ3 I-S-C_H loci are shown as arrows above the schematics. In the locus diagrams, the vertical lines indicate Hind III (H) sites. (A) B cells were unstimulated or activated, and B cell nuclei were analyzed in ChIP assays at the μ I-S-C_H locus by qPCR. Two to seven ChIP samples from each culture condition were derived from two independent experiments and were analyzed in duplicate and averaged, and SEMs are shown. (B) LPS-stimulated B cells were analyzed in ChIP assays at the γ3 I-S-C_H locus. Five ChIP samples from three independent experiments were analyzed. Samples from the RNAP II p-ser5 (H14) ChIP were concentrated sixfold and were analyzed in duplicate and averaged, and SEMs are shown. ND, not done.

WT locus the Iμ and Sμ-U or Sμ-D.2 sites are separated by 1.5 or 5.1 kb, respectively (Fig. 8 B). The total RNAP II density profile for the WT Iμ-Sμ-Cμ locus was similar to that previously observed with increased RNAP II occupancy within the Sμ tandem repeats (Fig. 8 C). In the Iμ-Sμ-Cμ locus from Sμ Δ/Δ B cells, RNAP II occupancy is relatively high at Cμ-U but is not enriched at Cμ-D compared with Eμ or Iμ (Fig. 8 C). Next, the effect of Sμ sequence on the pattern of H3K4me3 deposition in the Iμ-Cμ locus was examined. In the WT Iμ-Sμ-Cμ locus, the H3K4me3 modifications were highly enriched in the Iμ-Sμ interval (Figs. 3, 7 C, and 8 C). In Sμ Δ/Δ B cells, elevated levels of H3K4me3 marks are found at the Cμ-U site, as expected for a sequence located 0.73 kb distal to the TSS (Guenther et al., 2007), whereas at the Cμ-D site these modifications are strikingly depleted (Fig. 8 C). Thus, both the distance from the TSS and the unique sequence of the Sμ region determines the density of RNAP II occupancy and the deposition pattern of H3K4me3 modifications.

DISCUSSION

The mechanism by which AID attack is focused to transcriptionally active S regions but excluded from C_H genes within the same transcriptional unit has been unclear. In this study, we investigated whether transcription propagates differential chromatin accessibility across I-S-C_H loci by constructing detailed maps of chromatin accessibility, histone modifications, and RNAP II occupancy in vivo using RES and ChIP assays. Our data indicate that after transcription activation of GLTs, I-S regions are a focus for increased H3K4me3, H3Ac, and chromatin accessibility, whereas C_H regions accumulate the repressive countermarks H3K36me3 and H4K20me1, remain H3 hypo-Ac, and are inaccessible in chromatin. RES assays corroborate these findings and demonstrate that chromatin remodeling occurs at the 5′ and 3′ boarders of S regions but not in C_H regions. The bifurication of chromatin modifications within the I-S-C_H transcription unit corresponds well with zones targeted by or protected from AID attack.

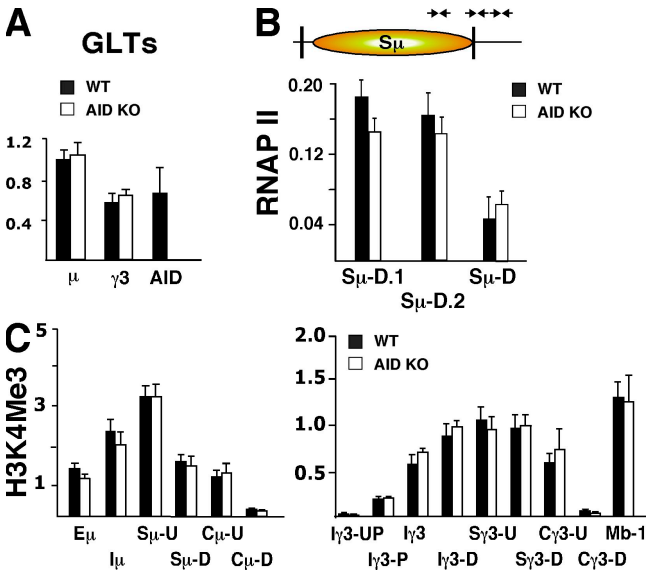

Figure 7. RNAP II p-ser5 stalling in S regions is independent of AID-induced DSBs. WT and AID-deficient (KO) B cells were stimulated with LPS for 48 h. (A) GLTs and AID expression were analyzed by qRT-PCR from WT and AID KO B cells. (B) WT and AID KO B cells were analyzed in ChIP assays for the μ I-S-C_H locus using antisera against total RNAP II. (C) ChIP analyses of the μ and γ3 I-S-C_H loci were performed using anti-H3K4me3 antisera. *Mb-1* primers were previously reported (Wang et al., 2006). (B and C) Data for ChIP assays from three to four samples derived from two independent experiments were analyzed in duplicate and averaged, and SEMs are shown.

Our TSA studies indicate that H3 Ac levels in S regions influence CSR frequency, confirming the physiological importance of this modification. Histone Ac may alter the net charge of nucleosomes and change the folding properties of the chromatin fiber, thereby promote DNA accessibility (Shahbazian and Grunstein, 2007), and may also create binding surfaces for specific protein–histone interactions (Li et al., 2007). A counterpoint to the directed hyper-Ac of S region is the relative deacetylation of the C_H regions. We also found that H3Ac and H3K4me3 distributions in I-S-C_H loci are superimposible. Recent evidence indicates that the H3K4me3 mark is directly bound by a protein constituent of the NuA3 HAT complex that functions to coordinate transcription activation with histone hyper-Ac (Taverna et al., 2006). In yeast, the H3K36me3 mark is targeted by the Rpd3S deactylase complex to reduce histone Ac and suppress inappropriate transcription initiation (Carrozza et al., 2005; Lieb and Clarke, 2005). Our TSA studies further demonstrate that HDAC inhibition has no impact on H3K4me3 levels or distribution, and does not lead to an unbridled spread of histone Ac from the S to C_H regions, as would be expected if histone Ac is independent of H3K4 Me. Thus, the underlying H3K4me3 and H3K36me3 Me pattern provides for recruitment of HATs and HDACs, respectively, which in turn regulate chromatin accessibility.

We propose a model whereby GLT expression is mechanistically linked to introduction of histone modifications and restructuring of chromatin in *Igh* loci. This model is based on the linkage between the phosphorylation status of RNAP II CTD, the recruitment of HMTs for H3K4me3 and H3K36me3, and the asymmetric Me of these residues in the promoter-proximal and 3′ coding regions of active genes in yeast and mammalian cells (Miller et al., 2001; Hampsey and Reinberg, 2003; Krogan et al., 2003; Ng et al., 2003; Carrozza et al., 2005; Guenther et al., 2005; Li et al., 2007). We conclude that chromatin modifications integrally linked to GLT expression are most likely responsible for constructing accessible and repressed chromatin environments coincident with S regions and C_H genes.

Detection of activating histone modifications throughout S regions that can extend >10 kb downstream of the GLT promoter is both surprising and unanticipated. Genome-wide analyses of histone marks in yeast and humans demonstrate that the activating modifications H3Ac and H3K4me3 are located promoter proximal and rarely extend more than 1 kb downstream

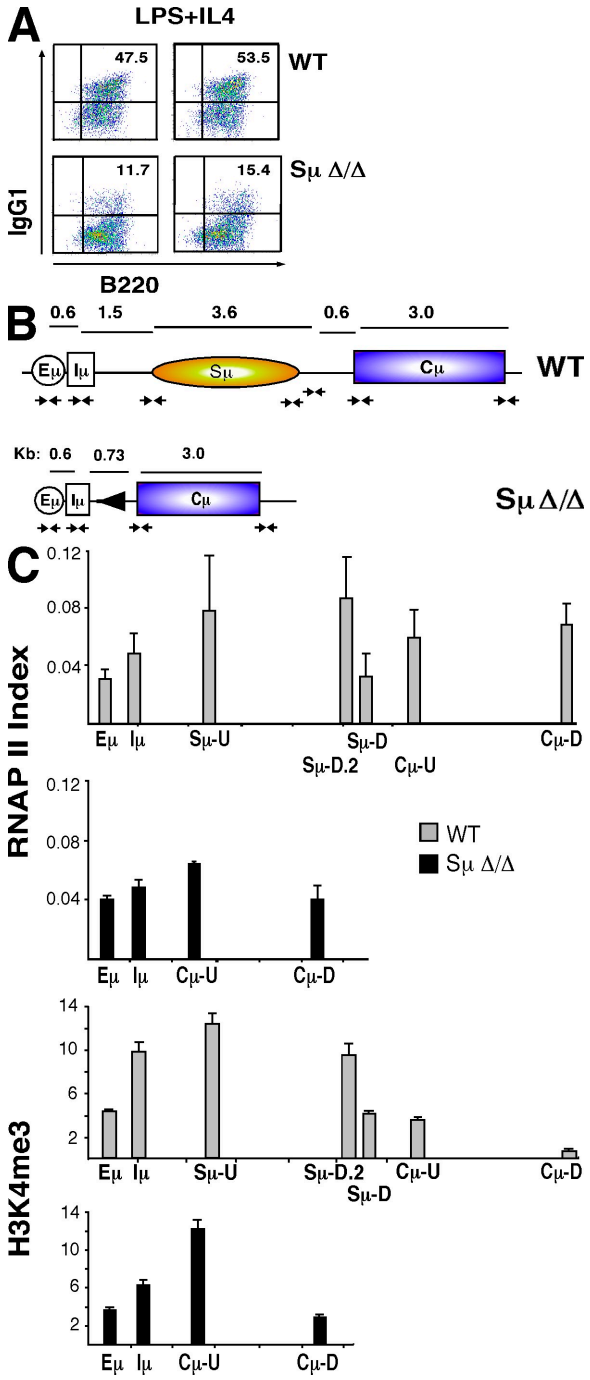

Figure 8. S region sequence directs RNAP II p-ser5 stalling and the deposition pattern of H3K4me3 marks. (A) FACS analysis using anti-B220 and anti-IgG1 was performed on WT and Sμ Δ/Δ B cells stimulated with LPS+IL-4 for 5 d (percentages are shown). (B) A schematic diagram depicting the Iμ-Cμ interval in WT and Sμ Δ/Δ mice is shown, and the position of primer pairs for each locus is indicated below the line by the arrows. Distances (kb) between primer pairs are indicated above each diagram. (C) B cells were stimulated with LPS+IL-4 for 48 h and analyzed in the μ I-S-C_H locus by ChIP assays using antisera against total RNAP II or anti-H3K4me3, as indicated. Data from two to five samples derived from two independent experiments were analyzed in duplicate and averaged, and SEMs are shown.

of the promoter (Bernstein et al., 2005; Pokholok et al., 2005). What directs the generation of chromatin hyperaccessibility long distances from the GLT promoters in the *Igh* locus? Based on the observation that the interaction between the initiating form of RNAP II (p-ser5) and the H3K4 HMT targets H3K4me3 to the 5′ end of active genes (Hampsey and Reinberg, 2003; Bernstein et al., 2005; Pokholok et al., 2005), we examined RNAP II occupancy of S regions. We reasoned that S region secondary structure or transcription-dependent R-loops might impede RNAP II elongation, thereby creating high occupancy of RNAP II together with its ancillary partners including HMTs, which could lay down the H3K4me3 mark. Our RNAP II ChIP studies demonstrate a significant enrichment of RNAP II p-ser5 in the Sμ and Sγ3 regions. Strikingly, in B cells devoid of Sμ DNA, RNAP II occupancy was not enriched in distal regions and H3K4me3 marks remained promoter proximal, demonstrating that S region sequence facilitates retention of RNAP II p-ser5 and is correlated with an extended zone of H3K4me3 modification. Although chromosomal breaks inhibit transcription by RNAP I (Kruhlak et al., 2007), our studies indicate that RNAP II p-ser5 enrichment is not related to the presence of DSBs in S DNA because occupancy is equivalent in WT and AID-deficient B cells in which DSBs are absent. Collectively, the data demonstrate that the S region sequences determine their own extended zone of chromatin remodeling and accessibility.

There are several possible mechanisms by which RNAP II is retained in S regions. Transcribed S regions contain R loops that are thought to provide single-stranded DNA stretches as substrate for AID deamination and thereby enhance the efficiency of CSR (Yu et al., 2003; Huang et al., 2007). Interestingly, RNA-DNA hybrid structures in R-loops impede transcription elongation (Huertas and Aguilera, 2003; Tous and Aguilera, 2007). S regions may also be subject to formation of G-loops that form as a consequence of combined G-quartet (Duquette et al., 2004) and R-loop structures and stall RNAP II transcription (Tornaletti et al., 2008). G-quartet structures are linked to G-rich sequences and have been noted in S regions, telomers, centromeres, and mutational hotspots, as well as in some triplet repeat expansion diseases (Phan et al., 2006). Although R-loops have been observed in S regions undergoing CSR in vivo (Yu et al., 2003; Huang et al., 2007), G-quartet structures have not been directly observed in similar circumstances (Roy et al., 2008). Interestingly, a broad and continuous distribution of H3K4me3 is found across multiple Hox-coding and intergenic regions, and is correlated with the RNAP II transcription of noncoding RNAs (Bernstein et al., 2005; Guenther et al., 2005). Similarly, antisense RNAs have been detected immediately 5′ of transcriptionally active S regions (Perlot et al., 2008). It is possible that antisense RNA expression from multiple initiating foci within the S regions create functionally alternative promoter sites across the S region that attract RNAP II and collectively recruit the H3K4 HMT. Additional studies are required to determine whether R-loop structures, G-quartets, or antisense RNA expression are causally linked to elevated RNAP II occupancy and deposition of H3K4me3 marks in S regions.

MATERIALS AND METHODS

Mice, cell culture, RT-PCR, and DC-PCR. C57B6 and C57B6 × 129 ($AID^{+/+}$) mice were purchased from the Jackson Laboratory. $AID^{-/-}$ mice (Muramatsu et al., 2000) were a gift from T. Honjo (Kyoto University, Kyoto, Japan). All mice were bred and housed under specific pathogen-free conditions, and animal protocols used in this study were approved by the Institutional Animal Care Committee of the University of Illinois College of Medicine. Single-cell suspensions of splenocytes from 8–12-wk-old mice were enriched for B or T cells and cultured as previously described (Wuerffel et al., 2007). 1B4.B6 cells were activated to undergo CSR as previously described (Wang et al., 2006). RNA was prepared with TRIzol (Invitrogen) according to the manufacturer's instructions. Semiquantitative and quantitative real-time RT-PCR (qRT-PCR) for GLTs, PSTs, *Gapd*, and *Aicda* transcripts were performed as previously described (Wang et al., 2006; Wuerffel et al., 2007). For semiquantitative RT-PCR, GLTs, PSTs, and IFN-γ PCR products were harvested after 33, 31, and 29 cycles. *Gapd* and *Hprt* PCR products were harvested after 30, 28, and 26 cycles.

ChIP and real-time qPCR. ChIP histone assays were performed as previously described (Wang et al., 2006). Immunoprecipitation was performed with anti-H3K9,14Ac (Millipore), anti-H3K36Me3 (Millipore), anti-H3K4Me3 (Abcam), anti-H4K20Me1, anti-H4K20Me2 (a gift from T. Jenuwein, Research Institute of Molecular Pathology, Vienna, Austria), anti-H4K20Me3 (Abcam), anti-RNAP (Santa Cruz Biotechnology, Inc.), anti-RNAP CTD p-ser5 (H14; Covance), and control antibodies (Millipore). All ChIPs used protein A–agarose beads, with the exception of the H14 antibody immunoprecipitation, where the protein A beads were preincubated for 30 min at room temperature with a linker IgG to the IgM antibody (Jackson ImmunoResearch Laboratories), as previously described (Xiao et al., 2007). The samples were analyzed by qPCR, as previously described (Wang et al., 2006). New primer sequences are listed in Table I. SEMs were calculated using data from independent experiments. p-values were calculated by using a single-tailed Student's *t* test.

RES assays and ligation-mediated PCR. RES assays were performed as previously described (Weinmann et al., 1999) with modifications. Nuclei were prepared from cultured cells or 5×10^6 stimulated lymphocytes, and were washed with 1× C1 buffer (1% Triton X-100, 50 mM $MgCl_2$, 100 mM Tris-HCl [pH 7.1], 11% sucrose) and then resuspended in 300 µl Hind III digestion buffer (Fermentas). Digestion reactions were initiated with 20 U Hind III at 37°C and performed for 1, 5, and 15 min, and were then stopped and treated with proteinase K, as previously described (Weinmann et al., 1999). 3 µg of genomic DNA from Hind III–treated nuclei was ligated with Hind III linkers (Oligo L.1 and L.2; Table I) in a 100-µl reaction overnight at 16°C. Linker-ligated DNA was purified and dissolved in 20 µl Tris EDTA. The first-round PCR was performed in 25-µl reactions with 1 µl DNA, 2 mM $MgCl_2$, 400 mM of each dNTP, 0.4 mM of each primer, and 1.5 U Platinum Taq (Invitrogen) with a linker-specific primer (Oligo L.1) and a locus-specific primer. The second round of nested PCR was performed in the presence of 1.5 mM $MgCl_2$ with 0.3 ml α-[^{32}P]dCTP (3,000 Ci/mmol) for 26 cycles. Radioactively labeled PCR products were resolved by 6% TBE PAGE and quantitated using a Storm 860 and ImageQuant software (GE Healthcare). The standard curve and linear range of PCR amplification were determined by a serial-diluted genomic DNA that is cut to completion and ligated. Samples were also normalized to *Gapd* for DNA content. Data are presented with the SEMs, and p-values were calculated using a single-tailed Student's *t* test.

We thank Dr. T. Honjo for the $AID^{-/-}$ mice and Dr. T. Jenuwein for the anti-H4K20me1 antisera.

This work was supported by the National Institutes of Health (grant RO1AI052400 to A.L. Kenter).

The authors declare that they have no competing financial interests.

Submitted: 30 July 2008
Accepted: 19 June 2009

REFERENCES

Alt, F.W., N. Rosenberg, V. Enea, E. Siden, and D. Baltimore. 1982. Multiple immunoglobulin heavy-chain gene transcripts in Abelson murine leukemia virus-transformed lymphoid cell lines. *Mol. Cell. Biol.* 2:386–400.

Bannister, A.J., R. Schneider, F.A. Myers, A.W. Thorne, C. Crane-Robinson, and T. Kouzarides. 2005. Spatial distribution of di- and tri-methyl lysine 36 of histone H3 at active genes. *J. Biol. Chem.* 280:17732–17736.

Barski, A., S. Cuddapah, K. Cui, T.Y. Roh, D.E. Schones, Z. Wang, G. Wei, I. Chepelev, and K. Zhao. 2007. High-resolution profiling of histone methylations in the human genome. *Cell.* 129:823–837.

Bernstein, B.E., M. Kamal, K. Lindblad-Toh, S. Bekiranov, D.K. Bailey, D.J. Huebert, S. McMahon, E.K. Karlsson, E.J. Kulbokas 3rd, T.R. Gingeras, S.L. Schreiber, and E.S. Lander. 2005. Genomic maps and comparative analysis of histone modifications in human and mouse. *Cell.* 120:169–181.

Carrozza, M.J., B. Li, L. Florens, T. Suganuma, S.K. Swanson, K.K. Lee, W.J. Shia, S. Anderson, J. Yates, M.P. Washburn, and J.L. Workman. 2005. Histone H3 methylation by Set2 directs deacetylation of coding regions by Rpd3S to suppress spurious intragenic transcription. *Cell.* 123:581–592.

Chaudhuri, J., U. Basu, A. Zarrin, C. Yan, S. Franco, T. Perlot, B. Vuong, J. Wang, R.T. Phan, A. Datta, et al. 2007. Evolution of the immunoglobulin heavy chain class switch recombination mechanism. *Adv. Immunol.* 94:157–214.

Duquette, M.L., P. Handa, J.A. Vincent, A.F. Taylor, and N. Maizels. 2004. Intracellular transcription of G-rich DNAs induces formation of G-loops, novel structures containing G4 DNA. *Genes Dev.* 18:1618–1629.

Gritzmacher, C.A. 1989. Molecular aspects of heavy-chain class switching. *Crit. Rev. Immunol.* 9:173–200.

Groth, A., W. Rocha, A. Verreault, and G. Almouzni. 2007. Chromatin challenges during DNA replication and repair. *Cell.* 128:721–733.

Guenther, M.G., R.G. Jenner, B. Chevalier, T. Nakamura, C.M. Croce, E. Canaani, and R.A. Young. 2005. Global and Hox-specific roles for the MLL1 methyltransferase. *Proc. Natl. Acad. Sci. USA.* 102:8603–8608.

Guenther, M.G., S.S. Levine, L.A. Boyer, R. Jaenisch, and R.A. Young. 2007. A chromatin landmark and transcription initiation at most promoters in human cells. *Cell.* 130:77–88.

Hampsey, M., and D. Reinberg. 2003. Tails of intrigue: phosphorylation of RNA polymerase II mediates histone methylation. *Cell.* 113:429–432.

Huang, F.T., K. Yu, B.B. Balter, E. Selsing, Z. Oruc, A.A. Khamlichi, C.L. Hsieh, and M.R. Lieber. 2007. Sequence dependence of chromosomal R-loops at the immunoglobulin heavy-chain Smu class switch region. *Mol. Cell. Biol.* 27:5921–5932.

Huertas, P., and A. Aguilera. 2003. Cotranscriptionally formed DNA:RNA hybrids mediate transcription elongation impairment and transcription-associated recombination. *Mol. Cell.* 12:711–721.

Kenter, A.L. 2005. Class switch recombination: an emerging mechanism. *Curr. Top. Microbiol. Immunol.* 290:171–199.

Khamlichi, A.A., F. Glaudet, Z. Oruc, V. Denis, M. Le Bert, and M. Cogne. 2004. Immunoglobulin class-switch recombination in mice devoid of any S mu tandem repeat. *Blood.* 103:3828–3836.

Kolasinska-Zwierz, P., T. Down, I. Latorre, T. Liu, X.S. Liu, and J. Ahringer. 2009. Differential chromatin marking of introns and expressed exons by H3K36me3. *Nat. Genet.* 41:376–381.

Kouzarides, T. 2007. Chromatin modifications and their function. *Cell.* 128:693–705.

Krogan, N.J., J. Dover, A. Wood, J. Schneider, J. Heidt, M.A. Boateng, K. Dean, O.W. Ryan, A. Golshani, M. Johnston, et al. 2003. The Paf1 complex is required for histone H3 methylation by COMPASS and Dot1p: linking transcriptional elongation to histone methylation. *Mol. Cell.* 11:721–729.

Kruhlak, M., E.E. Crouch, M. Orlov, C. Montano, S.A. Gorski, A. Nussenzweig, T. Misteli, R.D. Phair, and R. Casellas. 2007. The ATM repair pathway inhibits RNA polymerase I transcription in response to chromosome breaks. *Nature.* 447:730–734.

Kuzin, I.I., G.D. Ugine, D. Wu, F. Young, J. Chen, and A. Bottaro. 2000. Normal isotype switching in B cells lacking the I mu exon splice donor site: evidence for multiple I mu-like germline transcripts. *J. Immunol.* 164:1451–1457.

Li, B., M. Carey, and J.L. Workman. 2007. The role of chromatin during transcription. *Cell.* 128:707–719.

Lieb, J.D., and N.D. Clarke. 2005. Control of transcription through intragenic patterns of nucleosome composition. *Cell*. 123:1187–1190.

Luby, T.M., C.E. Schrader, J. Stavnezer, and E. Selsing. 2001. The mu switch region tandem repeats are important, but not required, for antibody class switch recombination. *J. Exp. Med*. 193:159–168.

Ma, L., H. Wortis, and A.L. Kenter. 2002. Two new isotype specific switching factors detected for Ig class switching. *J. Immunol*. 168:2835–2846.

Manis, J.P., M. Tian, and F.W. Alt. 2002. Mechanism and control of class-switch recombination. *Trends Immunol*. 23:31–39.

Miller, T., N.J. Krogan, J. Dover, H. Erdjument-Bromage, P. Tempst, M. Johnston, J.F. Greenblatt, and A. Shilatifard. 2001. COMPASS: a complex of proteins associated with a trithorax-related SET domain protein. *Proc. Natl. Acad. Sci. USA*. 98:12902–12907.

Muramatsu, M., K. Kinoshita, S. Fagarasan, S. Yamada, Y. Shinkai, and T. Honjo. 2000. Class switch recombination and hypermutation require activation-induced cytidine deaminase (AID), a potential RNA editing enzyme. *Cell*. 102:553–563.

Muse, G.W., D.A. Gilchrist, S. Nechaev, R. Shah, J.S. Parker, S.F. Grissom, J. Zeitlinger, and K. Adelman. 2007. RNA polymerase is poised for activation across the genome. *Nat. Genet*. 39:1507–1511.

Nelson, K.J., J. Haimovich, and R.P. Perry. 1983. Characterization of productive and sterile transcripts from the immunoglobulin heavy-chain locus: processing of micron and muS mRNA. *Mol. Cell. Biol*. 3:1317–1332.

Ng, H.H., F. Robert, R.A. Young, and K. Struhl. 2003. Targeted recruitment of Set1 histone methylase by elongating Pol II provides a localized mark and memory of recent transcriptional activity. *Mol. Cell*. 11:709–719.

Perlot, T., G. Li, and F.W. Alt. 2008. Antisense transcripts from immunoglobulin heavy-chain locus V(D)J and switch regions. *Proc. Natl. Acad. Sci. USA*. 105:3843–3848.

Phan, A.T., V. Kuryavyi, and D.J. Patel. 2006. DNA architecture: from G to Z. *Curr. Opin. Struct. Biol*. 16:288–298.

Pokholok, D.K., C.T. Harbison, S. Levine, M. Cole, N.M. Hannett, T.I. Lee, G.W. Bell, K. Walker, P.A. Rolfe, E. Herbolsheimer, et al. 2005. Genome-wide map of nucleosome acetylation and methylation in yeast. *Cell*. 122:517–527.

Rao, B., Y. Shibata, B.D. Strahl, and J.D. Lieb. 2005. Dimethylation of histone H3 at lysine 36 demarcates regulatory and nonregulatory chromatin genome-wide. *Mol. Cell. Biol*. 25:9447–9459.

Roy, D., K. Yu, and M.R. Lieber. 2008. Mechanism of R-loop formation at immunoglobulin class switch sequences. *Mol. Cell. Biol*. 28:50–60.

Saunders, A., L.J. Core, and J.T. Lis. 2006. Breaking barriers to transcription elongation. *Nat. Rev. Mol. Cell Biol*. 7:557–567.

Shahbazian, M.D., and M. Grunstein. 2007. Functions of site-specific histone acetylation and deacetylation. *Annu. Rev. Biochem*. 76:75–100.

Talasz, H., H.H. Lindner, B. Sarg, and W. Helliger. 2005. Histone H4-lysine 20 monomethylation is increased in promoter and coding regions of active genes and correlates with hyperacetylation. *J. Biol. Chem*. 280:38814–38822.

Taverna, S.D., S. Ilin, R.S. Rogers, J.C. Tanny, H. Lavender, H. Li, L. Baker, J. Boyle, L.P. Blair, B.T. Chait, et al. 2006. Yng1 PHD finger binding to H3 trimethylated at K4 promotes NuA3 HAT activity at K14 of H3 and transcription at a subset of targeted ORFs. *Mol. Cell*. 24:785–796.

Tornaletti, S., S. Park-Snyder, and P.C. Hanawalt. 2008. G4-forming sequences in the non-transcribed DNA strand pose blocks to T7 RNA polymerase and mammalian RNA polymerase II. *J. Biol. Chem*. 283:12756–12762.

Tous, C., and A. Aguilera. 2007. Impairment of transcription elongation by R-loops in vitro. *Biochem. Biophys. Res. Commun*. 360:428–432.

Vakoc, C.R., M.M. Sachdeva, H. Wang, and G.A. Blobel. 2006. A profile of histone lysine methylation across transcribed mammalian chromatin. *Mol. Cell. Biol*. 26:9185–9195.

Wade, J.T., and K. Struhl. 2008. The transition from transcriptional initiation to elongation. *Curr. Opin. Genet. Dev*. 18:130–136.

Wang, L., N. Whang, R. Wuerffel, and A.L. Kenter. 2006. AID-dependent histone acetylation is detected in immunoglobulin S regions. *J. Exp. Med*. 203:215–226.

Weinmann, A.S., S.E. Plevy, and S.T. Smale. 1999. Rapid and selective remodeling of a positioned nucleosome during the induction of IL-12 p40 transcription. *Immunity*. 11:665–675.

Wuerffel, R., L. Wang, F. Grigera, J. Manis, E. Selsing, T. Perlot, F.W. Alt, M. Cogne, E. Pinaud, and A.L. Kenter. 2007. S/S synapsis during class switch recombination is promoted by distantly located transcriptional regulatory elements and AID. *Immunity*. 27:711–722.

Xiao, T., Y. Shibata, B. Rao, R.N. Laribee, R. O'Rourke, M.J. Buck, J.F. Greenblatt, N.J. Krogan, J.D. Lieb, and B.D. Strahl. 2007. The RNA polymerase II kinase Ctk1 regulates positioning of a 5′ histone methylation boundary along genes. *Mol. Cell. Biol*. 27:721–731.

Youdell, M.L., K.O. Kizer, E. Kisseleva-Romanova, S.M. Fuchs, E. Duro, B.D. Strahl, and J. Mellor. 2008. Roles for Ctk1 and Spt6 in regulating the different methylation states of histone H3 lysine 36. *Mol. Cell. Biol*. 28:4915–4926.

Yu, K., F. Chedin, C.L. Hsieh, T.E. Wilson, and M.R. Lieber. 2003. R-loops at immunoglobulin class switch regions in the chromosomes of stimulated B cells. *Nat. Immunol*. 4:442–451.

Zeitlinger, J., A. Stark, M. Kellis, J.W. Hong, S. Nechaev, K. Adelman, M. Levine, and R.A. Young. 2007. RNA polymerase stalling at developmental control genes in the *Drosophila melanogaster* embryo. *Nat. Genet*. 39:1512–1516.